# The N-Terminal Flanking Region Modulates the Actin Binding Affinity of the Utrophin Tandem Calponin-Homology Domain

Surinder M. Singh,[†] Swati Bandi,[†] and Krishna M. G. Mallela*,[†,‡]

[†]Department of Pharmaceutical Sciences, Skaggs School of Pharmacy and Pharmaceutical Sciences, and [‡]Program in Structural Biology and Biochemistry, University of Colorado Anschutz Medical Campus, 12850 East Montview Boulevard, MS C238, Aurora, Colorado 80045, United States

S *Supporting Information*

ABSTRACT: Despite sharing a high degree of sequence similarity, the tandem calponin-homology (CH) domain of utrophin binds to actin 30 times stronger than that of dystrophin. We have previously shown that this difference in actin binding affinity could not be ascribed to the differences in inter-CH-domain linkers [Bandi, S., et al. (2015) *Biochemistry* 54, 5480−5488]. Here, we examined the role of the N-terminal flanking region. The utrophin tandem CH domain contains a 27-residue flanking region before its CH1 domain. We examined its effect by comparing the structure and function of full-length utrophin tandem CH domain Utr(1−261) and its truncated Utr(28−261) construct. Both full-length and truncated constructs are monomers in solution, with no significant differences in their secondary or tertiary structures. Truncated construct Utr(28−261) binds to actin 30 times weaker than that of the full-length Utr(1−261), similar to that of the dystrophin tandem CH domain with a much shorter flanking region. Deletion of the N-terminal flanking region stabilizes the CH1 domain. The magnitude of the change in binding free energy upon truncation is similar to that of the change in thermodynamic stability. The isolated N-terminal peptide by itself is significantly random coil and does not bind to F-actin in the affinity range of Utr(1−261) and Utr(28−261). These results indicate that the N-terminal flanking region significantly affects the actin binding affinity of tandem CH domains. This observation further stresses that protein regions other than the three actin-binding surfaces identified earlier, irrespective of whether they directly bind to actin, also contribute to the actin binding affinity of tandem CH domains.
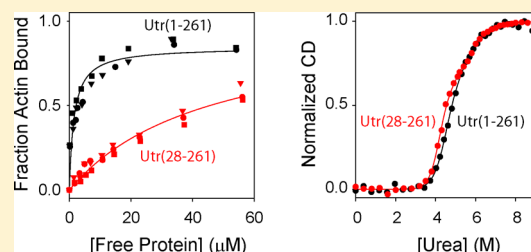
Tandem calponin-homology (CH) domains are the most common actin-binding domains in proteins, yet structural determinants of their actin binding are less understood.[1,2] Determining their structure−function relationship will improve our understanding of the triggering mechanisms of severe muscle diseases such as muscular dystrophy.[3] For example, mutations in the dystrophin tandem CH domain trigger Duchenne/Becker muscular dystrophy,[3] whereas mutations in the α-actinin tandem CH domain trigger glomerulosclerosis.[4] Shortened constructs of some of these proteins such as dystrophin and utrophin have been proposed for use in the gene therapy of muscular dystrophy;[5,6] however, these mini-dystrophins and mini-utrophins suffer from decreased stability, shortened in vivo half-life, and poorer function.[7−9] Therefore, to improve such gene and protein engineering efforts, we first need to identify the minimal protein regions required for the dystrophin and utrophin structure and function.

Previous work has identified three actin-binding surfaces (ABSs) with which tandem CH domains interact with actin.[10,11] Subsequent experiments with truncated protein constructs have indicated that the first two ABSs in the N-terminal CH1 domain play a major role in determining the actin binding affinity compared to the third ABS in the C-terminal CH2 domain.[12−17] These studies further implied that the actin binding affinity of dystrophin and utrophin tandem CH domains should be similar, because they have highly similar

ABSs and CH domains, which we found not to be true. Dystrophin and utrophin tandem CH domains share ∼82% similar sequences;[18] however, the utrophin tandem CH domain binds to actin ∼30 times stronger than that of dystrophin tandem CH domain.[16,17] To understand this puzzle, we have examined how the structural differences between utrophin and dystrophin tandem CH domains determine their differences in actin binding affinity. Similar to the full-length tandem CH domains, individual CH domains are also highly similar. The CH1 domains of dystrophin and utrophin are ∼88% similar in sequence, whereas the CH2 domains share 86% similar sequences.[19] However, dystrophin and utrophin tandem CH domains differ in terms of their relative orientation around the interdomain linker connecting the two CH domains.[19] The dystrophin tandem CH domain predominantly exists in a closed conformation with its two CH domains interacting with one another,[20] whereas the utrophin tandem CH domain predominantly exists in an open conformation with decreased inter-CH-domain interactions.[21] To examine whether these differences in interdomain linker account for the differences in their actin binding affinity, in our previous work, we swapped

the linker regions between dystrophin and utrophin tandem CH domains.[19] Linker swapping changed the actin binding affinity by 2-fold, but the changes in binding free energy are much lower by an order of magnitude compared to the corresponding changes in the thermodynamic stability of tandem CH domains, indicating that the linker region determines primarily the structural stability compared to the actin binding affinity.[19]

Because variation in the interdomain linker could not account for the differences in actin binding affinity,[19] we further examined the structures of various tandem CH domains. A sequence similarity comparison showed that some tandem CH domains have N-terminal flanking regions that are longer than others.[18,22] In this work, we examine how this N-terminal flanking region determines the actin binding affinity using the utrophin tandem CH domain as a model tandem CH domain. The utrophin tandem CH domain was chosen for this study for two reasons: (i) it has one of the longest flanking regions (27 residues) compared to others, and (ii) it exists in an open conformation with minimal inter-CH-domain interactions, so that we can probe the effect of the flanking region on CH1 binding to actin with minimal contribution from CH2. To test the effect of the N-terminal flanking region, we created a truncated construct containing residues 28−261, labeled as Utr(28−261), and compared its actin binding affinity and thermodynamic stability with that of the full-length tandem CH domain, Utr(1−261).

■ MATERIALS AND METHODS

Cloning, Expression, and Purification of Full-Length Utrophin Tandem CH Domain Utr(1−261) and Its Truncated Construct, Utr(28−261). Plasmid vectors for full-length utrophin tandem CH domain Utr(1−261) and its truncated construct, Utr(28−261), were cloned using the coding DNA in the pET-SUMO expression vector using BamHI and XhoI restriction endonuclease sites. The ligation mix was transformed into DH5α by heat shock. Plasmids were amplified using a Qiagen miniprep kit, and the constructs were confirmed by DNA sequencing. These were transformed into BL21(DE3) cells. Both Utr(1−261) and Utr(28−261) were expressed as soluble proteins and purified using Ni-His affinity chromatography. The N-terminal SUMO fragment was cleaved using Ulp1 protease,[23] and pure proteins were eluted in the flow-through using a Ni-His affinity column.

Synthesis and Labeling of Peptide Utr(1−27). The 27-residue peptide Utr(1−27) corresponding to the N-terminal flanking region of the utrophin tandem CH domain was synthesized by Biomatik Co. For measuring fluorescence anisotropy, this peptide was labeled with fluorescein isothiocyanate (FITC) at its N-terminus using aminohexanoic acid (Ahx) as the linker.

Circular Dichroism (CD). Utr(1−261), Utr(28−261), and Utr(1−27) (protein concentration of 1 μM) in phosphate-buffered saline (PBS) [100 mM NaH$_2$PO$_4$ and 150 mM NaCl (pH 7)] were used for measuring CD (Chirascan Plus, Applied Photophysics, Leatherhead, U.K.). The mean residue ellipticity (MRE) was calculated from the CD values in millidegrees.[24]

Fluorescence. Fluorescence spectra of native (1 μM in PBS buffer) and unfolded states (1 μM in PBS buffer containing 8 M urea) of Utr(1−261) and Utr(28−261) were recorded by exciting the samples at 280 nm (PTI QuantaMaster Fluorimeter).

Analytical Ultracentrifugation (AUC). Utr(1−261) and Utr(28−261) (20 μM each) were subjected to sedimentation velocity AUC in PBS buffer at 50000 rpm using a Beckman XL-A analytical ultracentrifuge. The absorbance at 280 nm was used to record the meniscus shift data. Raw data were analyzed using SEDFIT. The density and viscosity of the buffer were calculated using SEDNTERP. Data were fitted to a continuous sedimentation distribution model.

Dynamic Light Scattering (DLS). Oligomerization of the full-length tandem CH domain and CH2 was checked using DLS. Both proteins (50 μM in PBS buffer) were subjected to a zeta-sizer (Nano ZS, Malvern). An average of 11 runs were used for the calculation of the mean diameter.

Denaturant Melts. For urea denaturation melts of Utr(1−261) and Utr(28−261), 1 μM protein in PBS buffer was used. Changes in the far-UV CD signal at 222 nm and the intrinsic protein fluorescence of aromatic amino acids (excitation at 280 nm, emission at 360 nm) were monitored as a function of an increasing urea concentration. Because the CD melt of Utr(28−261) showed a clear double-sigmoidal transition, these four denaturant melts [CD and fluorescence melts of Utr(1−261) and CD and fluorescence melts of Utr(28−261)] were globally fitted to a three-state linear extrapolation unfolding model,[25] described below.

$$S_D = \left[(S_N + m_N[D]) + (S_I + m_I[D])e^{-(\Delta G_{NI}+m_{NI}[D])/RT} \right.$$
$$+ \left. (S_U + m_U[D])e^{-(\Delta G_{NI}+m_{NI}[D])/RT}e^{-(\Delta G_{IU}+m_{IU}[D])/RT} \right]$$
$$/\left[1 + e^{-(\Delta G_{NI}+m_{NI}[D])/RT} + e^{-(\Delta G_{NI}+m_{NI}[D])/RT} \right.$$
$$\left. e^{-(\Delta G_{IU}+m_{IU}[D])/RT} \right] \tag{1}$$

where S_D is the measured signal as a function of denaturant concentration [D]; S_N, S_I, and S_U are the intrinsic signals corresponding to the native, intermediate, and unfolded states, respectively, in the absence of denaturant; m_N, m_I, and m_U are the slopes of the linear dependence of S_N, S_I, and S_U, respectively, on denaturant concentration; ΔG_{NI} and ΔG_{IU} correspond to the Gibbs free energies of the first (N ↔ I) and second (I ↔ U) transitions, respectively, in the absence of denaturant; and m_{NI} and m_{IU} correspond to the slopes of the linear dependence of ΔG_{NI} and ΔG_{IU}, respectively, with denaturant concentration.

Equation 1 indicates that the three-state fit of a denaturant melt involves 10 fit parameters, specifically, S_N, m_N, S_I, m_I, S_U, m_U, ΔG_{NI}, m_{NI}, ΔG_{IU}, and m_{IU}. Therefore, to minimize the number of fit parameters, we assumed that the CD signals of the native state, the unfolded state, and the intermediate do not change with urea concentration, which is evident from the flat native and unfolded baselines in the CD melts. Because the partially unfolded intermediate consists of the unfolded CH1 domain and the the folded CH2 domain,[26] the CD signal of the intermediate is assumed to be half of that of the native and unfolded states. These two assumptions may not be valid in the case of denaturant melts measured by fluorescence, because the fluorescence baseline of the native and unfolded states showed a weak linear dependence on denaturant concentration. In addition, the fluorescence signal of the intermediate state may not be half of that of the native and unfolded states, because the change in the fluorescence signal may not mirror the equivalent change in the protein's structure.[27,28] Fluorescence signals
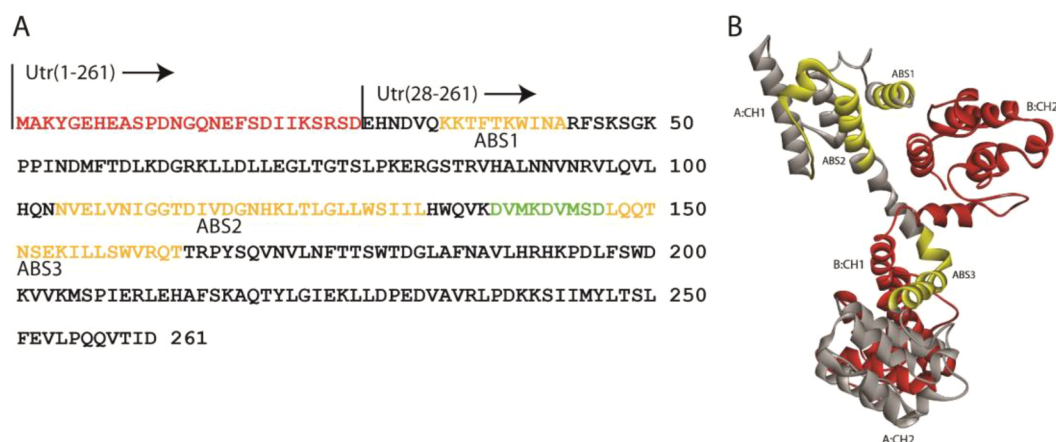
Figure 1. (A) Amino acid sequence of utrophin tandem CH domain Utr(1−261). This figure also shows the N-terminal flanking region (red), three actin-binding surfaces (ABSs) (yellow), the interdomain linker connecting the two CH domains (green), and the sequence of truncated construct Utr(28−261). (B) X-ray crystal structure of truncated utrophin tandem CH domain Utr(28−261) (Protein Data Bank entry 1QAG). Although this domain has been shown to be a monomer in solution, it crystallizes as an antiparallel, domain-swapped dimer. The two monomers, labeled A and B, are colored gray and red, respectively. The three ABSs are colored yellow in monomer A.

depend primarily on the solvent environment and the nearby chemical groups that quench the fluorescence.

The main goal of the three-state analysis described above is to determine how the N-terminal flanking region affects the stability of the CH1 domain, which determines the actin binding affinity of the tandem CH domains. Because the utrophin tandem CH domain predominantly exists in an open conformation with no interactions between the two CH domains, we assumed that the N-terminal flanking region that occurs before the CH1 domain does not affect the stability of the CH2 domain. This assumption may not be valid in the case of the other tandem CH domain, such as that of dystrophin, which exists in a closed conformation with significant inter-CH-domain interactions where the N-terminal regions of CH1 interact with the CH2 domain.[20]

Actin Binding Affinity of Utr(1−261) and Utr(28−261). Skeletal muscle G-actin (Cytoskeleton, Denver, CO) was polymerized (7 μM) and incubated with varying concentrations of the binding partner protein [Utr(1−261) or Utr(28−261)] for 1 h at room temperature. The mixture described above (final volume of 100 μL) was centrifuged at 100000g for 30 min (sw55Ti rotor, Beckman Optima LE80K), and pellets were solubilized in 30 μL of sodium dodecyl sulfate−polyacrylamide gel electrophoresis (SDS−PAGE) loading buffer. Half of this was boiled and subjected to SDS−PAGE and stained with Coomassie blue. The intensity of the individual bands was determined using Image Lab version 5.2 on a Bio-Rad Gel Doc XR instrument. Intensity values for actin bands were corrected by multiplying with the correction factors obtained from the BSA standard curve to account for the differential staining of the dye to proteins.[17,29,30] The ratio of the band intensities was used to determine the fraction bound of F-actin using the formula fraction bound = (corrected band intensity of bound protein × molecular weight of actin)/(corrected band intensity of actin × molecular weight of bound protein). The free protein concentration was calculated using the formula free protein = total protein added − (fraction actin bound × concentration of total actin added). The binding data were fit to the equation

$$\text{fraction actin bound} = B_{max}x/(K_d + x) \qquad (2)$$

where x is the free protein concentration, B_{max} is the maximal number of binding sites, and K_d is the dissociation constant.[30]

Actin Binding Affinity of 27-Residue Peptide Utr(1−27). Changes in the steady-state fluorescence anisotropy of labeled peptide Utr(1−27) were measured at a fixed concentration of the peptide (2 μM) and varying concentrations of F-actin. The excitation and emission wavelengths were 508 and 530 nm, respectively, corresponding to the FITC fluorophore. The fluorescence anisotropy of the peptide in 70% glycerol was used as a control to compare the significance of anisotropy changes.

FT-IR Spectroscopy. IR spectra of Utr(1−261) and Utr(28−261) (200 μM in PBS) were recorded using a Prota 3S FT-IR spectrometer and CaF2 cell (Biotools). For each sample, 128 scans were acquired in single-beam mode at 4 cm⁻¹ resolution. IR absorbance spectra were processed using GRAMS/AI 7.00 software (Thermo Galactic, Thermo Electron).

Raman Spectroscopy. Raman spectra of Utr(1−261) and Utr(28−261) (200 μM in PBS) were recorded using a Kaiser Raman RxN1 spectrometer (Kaiser Optical Systems, Ann Arbor, MI). A 785 nm laser with an approximately 280 mW laser power source was used. An approximately 110 μL sample was placed in a 3 mm × 3 mm quartz cuvette, which was then loaded into a Peltier temperature-controlled sample compartment. To avoid potential problems due to sample evaporation, the sample cuvette was tightly sealed with a Teflon stopper. Unless otherwise noted, Raman spectra were recorded with 12 co-additions of a 10 s exposure. The buffer spectrum was subtracted from the protein spectrum.

Time-Resolved Fluorescence Measurements. A time-correlated single-photon counting (TCSPC) setup on a Horiba Scientific DeltaFlex instrument was used to record time-resolved fluorescence intensity and anisotropy decays of 1 μM Utr(1−261), Utr(28−261), and Utr(1−27). For tryptophan fluorescence from Utr(1−261) and Utr(28−261), the samples were excited with a 300 nm UV light-emitting diode, and the emission was collected at 360 nm. For FITC fluorescence from labeled Utr(1−27), the samples were excited with a 508 nm pulsed laser diode, and the emission was collected at 530 nm.

■ RESULTS

Deletion of the N-Terminal Flanking Region Did Not Perturb the Secondary or Tertiary Structure of the Utrophin Tandem CH Domain. Amino acid sequences of the full-length tandem CH domain, Utr(1−261), and its truncated construct, Utr(28−261), are shown in Figure 1A. The purity of the proteins is shown in Figure 2A. Both proteins eluted as
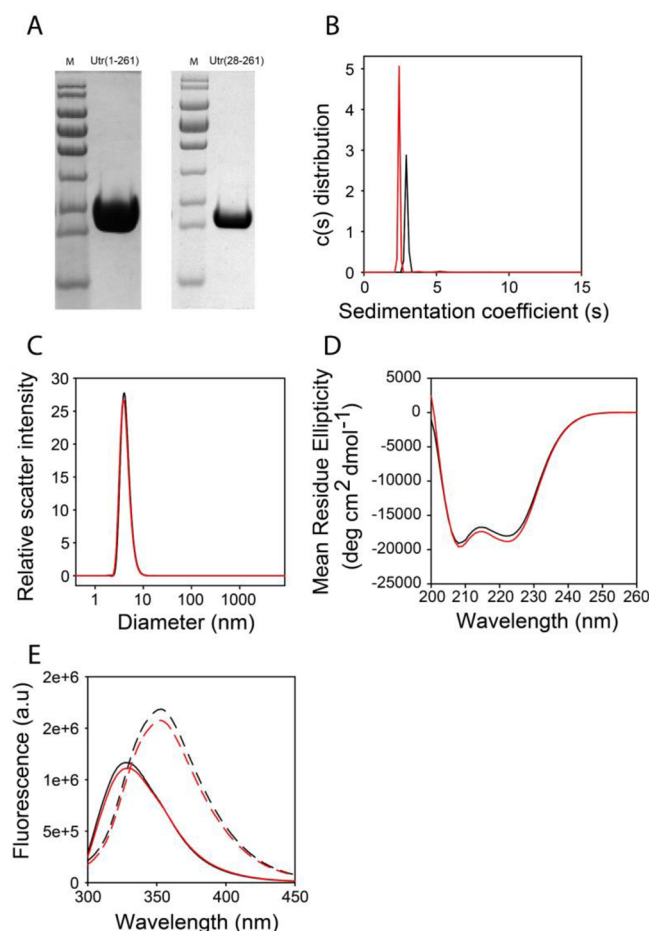

Figure 2. (A) SDS−PAGE of the purified full-length utrophin tandem CH domain, Utr(1−261), and its truncated construct, Utr(28−261). Lanes labeled M contained the molecular weight markers (17, 26, 34, 43, 56, 72, 95, 130, and 170 kDa from bottom to top, respectively). (B) Sedimentation coefficient distributions obtained from sedimentation velocity analytical ultracentrifugation (SV-AUC). (C) Scattering intensity profiles obtained from dynamic light scattering (DLS). (D) Far-UV circular dichroism (CD) spectra. (E) Fluorescence spectra of the native (solid) and unfolded (dashed) states. In panels B−E, black and red curves correspond to Utr(1−261) and Utr(28−261), respectively.

single bands on SDS−PAGE. Although Utr(28−261) crystallized as a dimer in earlier X-ray studies (Figure 1B), both Utr(1−261) and Utr(28−261) are monomers in solution. Analytical ultracentrifugation (AUC) (Figure 2B) and dynamic light scattering (DLS) (Figure 2C) experiments showed a single species. The molecular weights calculated from the sedimentation coefficients determined from AUC [Utr(1−261), 30 ± 2 kDa; Utr(28−261), 27 ± 2 kDa] matched with the estimated molecular weights from their amino acid sequences [Utr(1−261), 30 kDa; Utr(28−261), 27 kDa]. Consistent with the α-helical structure (Figure 1B), Utr(1−

261) showed a characteristic circular dichroism (CD) with negative bands at 208 and 222 nm (Figure 2D). Utr(28−261) showed a similar CD spectrum, indicating that the deletion of the N-terminal flanking region consisting of residues 1−27 did not significantly perturb the secondary structure of the protein. Minor differences in the amplitude of the CD signal between the two proteins can be explained because of the deletion of the N-terminal flanking region (discussed below in another section of Results). Deletion of the flanking region also did not perturb the tertiary structure of the protein, as evident in the lack of change in the intrinsic fluorescence spectra (Figure 2E). Because fluorescence originates from aromatic side chains, it is often considered as a probe of protein's tertiary structure. Native and unfolded states of Utr(1−261) emit fluorescence with maxima at 327 and 353 nm. The red shift in the fluorescence emission maximum upon protein unfolding is indicative of the burial of tryptophan residues in the core of the protein.[31] More importantly, the emission spectra of Utr(28−261) are similar to those of Utr(1−261) in both native and unfolded states, indicating no change in the tertiary structure upon deletion of the N-terminal flanking region.

Deletion of the N-Terminal Flanking Region Decreased the Actin Binding Affinity of the Utrophin Tandem CH Domain. We used co-sedimentation assays[15] to measure the actin binding affinities of Utr(1−261) and Utr(28−261). Panels A and B of Figure 3 show SDS−PAGE of the co-sedimented pellets that contained actin and actin-bound proteins. This experiment was performed at a fixed concentration of actin and varying concentrations of either Utr(1−261) or Utr(28−261). The protein band intensities on SDS−PAGE were quantified and corrected for the differential staining of the dye.[17,29] Figure 3C shows the actin binding curves for Utr(1−261) and Utr(28−261). Deletion of the N-terminal flanking region decreased the actin binding affinity of utrophin tandem CH domain by 30-fold. Fitting these binding curves resulted in K_d values of 1.53 ± 0.88 μM for Utr(1−261) and 45.52 ± 7.63 μM for Utr(28−261). The decreased actin binding affinity of truncated Utr(28−261) is similar to that of the dystrophin tandem CH domain (K_d = 47.05 ± 13.92 μM) whose flanking region is much shorter (nine residues).[16,19] These values clearly indicate that the N-terminal flanking region plays a significant role in determining the actin binding affinity of tandem CH domains.

Deletion of the N-Terminal Flanking Region Increased the Structural Stability of the CH1 Domain. Stabilities of Utr(1−261) and Utr(28−261) were measured using denaturant melts with urea as the denaturant (Figure 4). When unfolding was monitored using CD at 222 nm (Figure 4A), Utr(1−261) appears to be melted in a single cooperative, sigmoidal transition. However, unfolding of Utr(28−261) with urea clearly deviated from a single-sigmoidal transition; rather, it showed a double-sigmoidal transition corresponding to the unfolding of the two CH domains inferred previously.[26] Deletion of the N-terminal flanking region significantly affected the first transition corresponding to the unfolding of the CH1 domain, whereas the second transition corresponding to the CH2 unfolding was relatively unaffected. This is consistent with the open structure of the utrophin tandem CH domain with minimal inter-CH-domain interactions[21] (Figure 1B), because the flanking region occurs before the CH1 domain. Similar observations were also made when protein unfolding was monitored using changes in the protein fluorescence signal (Figure 4B).
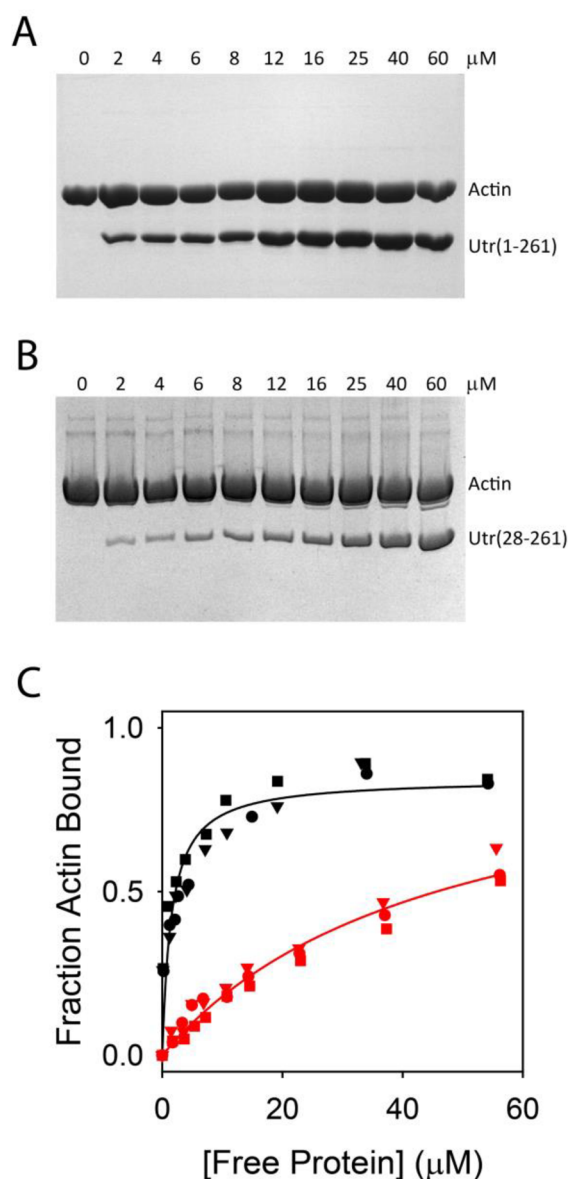
Figure 3. Actin binding of Utr(1−261) and Utr(28−261). (A and B) SDS−PAGE of the pellets from high-speed centrifugation performed at a fixed concentration of F-actin (7 μM) and with varying concentrations of either Utr(1−261) or Utr(28−261). (C) Actin binding curves obtained from the band intensities on SDS−PAGE shown in panels A and B, after correcting for differential staining of the dye to proteins. Circles, triangles, and rectangles represent the data from three independent repeats of the co-sedimentation assay. These binding curves were fit to determine the K_d and B_{max} values, listed in Table 1.

To obtain more quantitative information about the effect of the N-terminal flanking region, we globally analyzed the CD and fluorescence denaturant melts of both Utr(1−261) and Utr(28−261) to a three-state model with an intermediate between the native and unfolded states (eq 1 in Materials and Methods). The evidence of the presence of an intermediate state has been shown previously.[26] We assumed that the deletion of the flanking region did not affect the second transition, which is evident from the CD unfolding curves (Figure 4A and as discussed above). The validity of this assumption was also confirmed by three-state fitting of individual denaturant melts of Utr(1−261) and Utr(28−261),
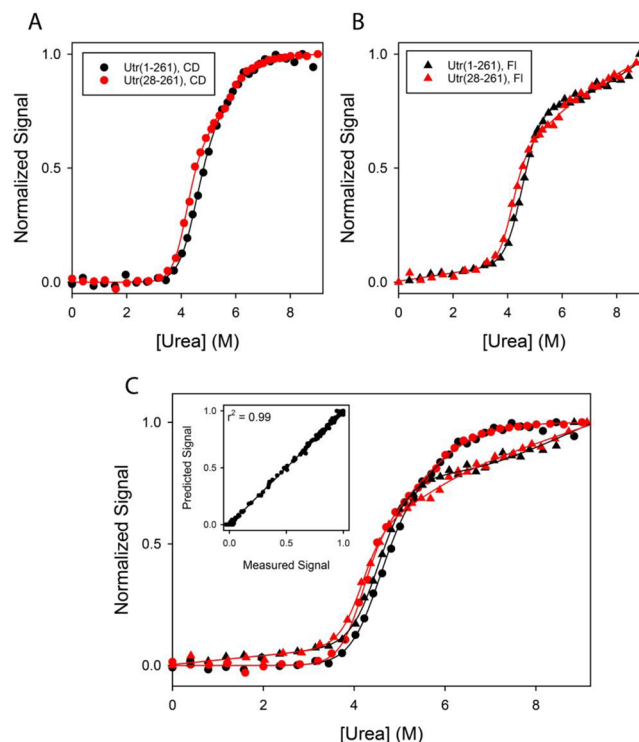
Figure 4. Structural stability of Utr(1−261) and Utr(28−261) probed using urea denaturant melts. Normalized changes in (A) the CD signal at 222 nm and (B) the intrinsic protein fluorescence of Utr(1−261) (black) and Utr(28−261) (red) as a function of an increasing urea concentration. (C) All the four denaturant melts in panels A and B were globally fitted to a three-state unfolding model assuming that the truncation did not affect the second sigmoidal transition corresponding to the unfolding of the CH2 domain. The fit parameters are listed in Table 1. The inset in panel C shows the quality of the fit in terms of how the fit parameters predict the experimentally measured signals.

and the fit parameters (Table S1) indicate that the change in the stability of CH2 is not statistically significant. Solid lines in panels A and B of Figure 4 indicate the three-state fit results from the global analysis of the denaturant melts of both Utr(1−261) and Utr(28−261), and the inset in Figure 4C shows the correlation between the predicted and measured values. The three-state model fits the data reasonably well. The fit results indicated a surprising result. Deletion of the N-terminal flanking region marginally stabilized the CH1 domain by $\Delta\Delta G_{NI} = 1.37 \pm 0.68$ kcal/mol. This stabilization of the CH1 domain upon deletion is counterintuitive to the appearance of the denaturant melts, which indicates that it unfolds at a lower denaturant concentration (Figure 4). However, because Gibbs free energy ΔG is a product of the midpoint denaturant concentration, C_m, and the slope of linear variation of ΔG_D with denaturant concentration, m-value,[32,33] the decrease in the midpoint denaturant concentration is compensated by a much larger increase in the m-value, resulting in an increase in the stability of the CH1 domain.

The Isolated N-Terminal Flanking Region Is Significantly Random Coil and Does Not Bind to F-Actin in the K_d Range of the CH1 or Tandem CH Domain. We further examined whether the isolated N-terminal flanking region of the utrophin tandem CH domain is structured and binds to actin by itself in the absence of the two CH domains. The CD spectrum of 27-residue peptide Utr(1−27) corresponding to the flanking region indicates that it is significantly random coil
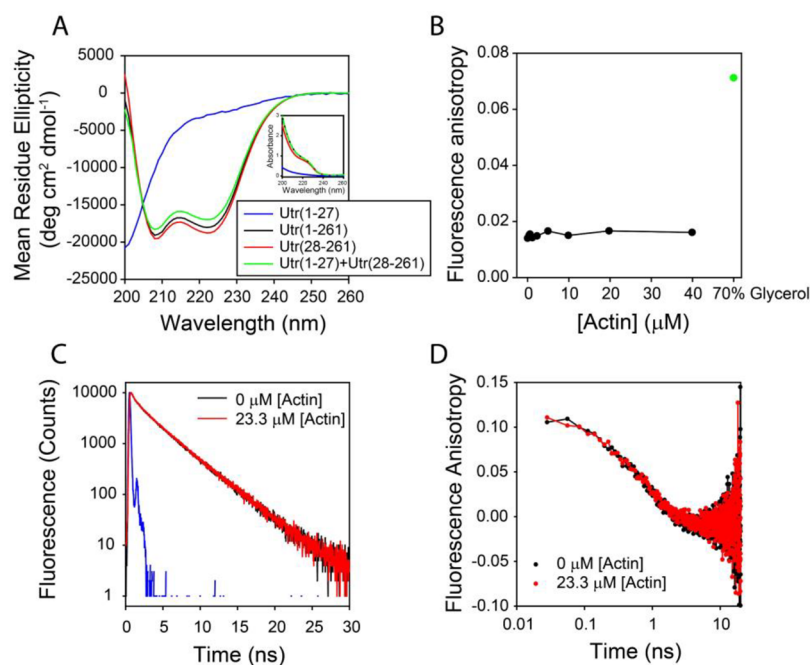
Figure 5. Structure and function of 27-residue isolated peptide Utr(1−27) corresponding to the N-terminal flanking region. (A) Circular dichroism (CD) spectrum of Utr(1−27) (blue) in comparison with the spectra of Utr(1−261) (black) and Utr(28−261) (red). The sum of the CD spectra of Utr(1−27) and Utr(28−261) (green) is not the same as that of Utr(1−261). The inset shows the corresponding absorption spectra, indicating that these differences in CD signals are not due to the differences in absorbance. (B) Actin binding of Utr(1−27) measured using the fluorescence anisotropy of the FITC dye attached to its N-terminus. Compared to that of the control (70% glycerol; green circle), the anisotropy did not show a significant increase with the increase in the actin concentration. (C) Time-resolved fluorescence intensity decays and (D) time-resolved anisotropy decays in the absence (black) and presence of actin (red). The blue curve in panel C is the instrument response function (IRF) of the time-resolved fluorescence instrument.

with minimal α-helical structure (Figure 5A), which is evident from the absence of negative peaks at 208 and 222 nm and the appearance of a negative peak below 200 nm. However, when it is part of the tandem CH domain, this peptide becomes structured. The CD spectral intensity of the full-length utrophin tandem CH domain, Utr(1−261), is higher than the sum of the CD signals of Utr(1−27) and Utr(28−261) (Figure 5A). This is not due to the differences in the absorbance intensities. Utr(1−261) has an absorption spectrum identical to that of the sum of Utr(1−27) and Utr(28−261) (inset of Figure 5A). Structuring of the N-terminal region upon linking to the tandem CH domain is also reflected in the increase in the 222 nm:208 nm ratio. The ratios were 0.96 ± 0.01 in the case of Utr(1−261) and 0.92 ± 0.01 for the sum of Utr(1−27) and Utr(28−261). These ratios are very close because the N-terminal flanking region is only 10% of the full-length utrophin tandem CH domain.

Traditional co-sedimentation assays (similar to Figure 3) could not be used to measure the actin binding of Utr(1−27), because it has a molecular weight much lower than that of Utr(1−261) or Utr(28−261). Because of its smaller size, the protein bands on SDS−PAGE will be more prone to error in digitization. Therefore, we used fluorescence anisotropy as an alternative method to measure its actin binding. If the peptide is restricted in its rotational diffusion upon binding to actin, its anisotropy will increase. The N-terminal amino acid of Utr(1−27) was labeled with a FITC fluorophore. We first tested whether the anisotropy of this fluorophore is sensitive to changes in rotational diffusion by examining the effect of solution viscosity using a 70% glycerol solution. Compared to that of the buffer, the fluorescence anisotropy increased to

0.071 from 0.014 (green dot in Figure 5B). For actin binding experiments, the peptide concentration was fixed at 7 μM, and actin was titrated from 0 to 40 μM. The peptide did not show significant changes in anisotropy compared to the 70% glycerol solution, which indicates that Utr(1−27) does not bind to actin in the K_d range of the CH1 domain. The absence of binding of the peptide to actin was also evident from time-resolved fluorescence intensity (Figure 5C) and anisotropy (Figure 5D) decays. Binding is expected to significantly change the solvent environment of the fluorophore. Time-resolved fluorescence is much more sensitive to local environments than steady-state fluorescence.[31] The fluorescence intensity decays were identical in the absence and presence of 23.3 μM actin, indicating the absence of Utr(1−27) binding to actin. Binding should slow the rotational correlation time or tumbling rate of the peptide. However, time-resolved anisotropy decays did not show any difference in the absence or presence of actin (Figure 5D), indicating that the peptide does not bind to actin in the K_d range of the CH1 or tandem CH domain.

The Presence of the N-Terminal Flanking Region Did Not Affect the Secondary or Tertiary Structures of the Utrophin Tandem CH Domain. As discussed before, no significant changes were observed in the CD or fluorescence spectra upon deletion of the N-terminal flanking region (Figures 2D,E and 5A), indicating that the N-terminal region does not significantly affect the secondary or tertiary structures of the utrophin tandem CH domain. To further confirm, we performed additional experiments (Figure 6). We used fluorescence quenching experiments using acrylamide as the quencher to probe whether any tertiary structural changes occur, resulting in the solvent exposure of tryptophan residues.
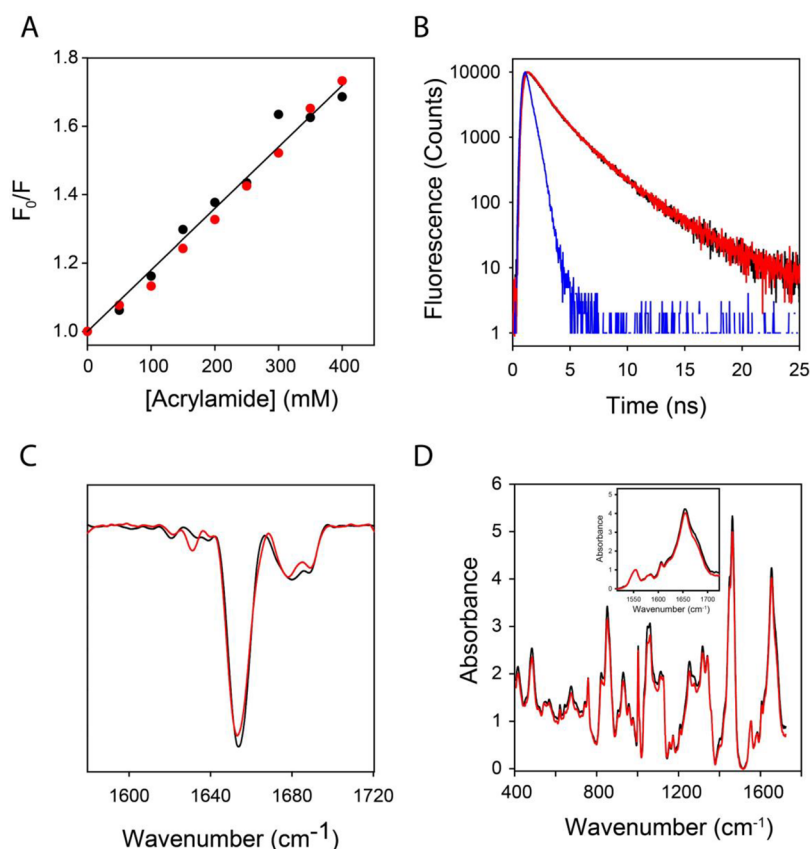
Figure 6. Effect of the N-terminal flanking region on the structure of the utrophin tandem CH domain. (A) Stern−Volmer plots of acrylamide quenching. (B) Time-resolved fluorescence intensity decays. (C) FT-IR spectra. (D) Raman vibrational spectra. Black and red curves correspond to Utr(1−261) and Utr(28−261), respectively. Similar to the CD and fluorescence spectra (Figure 2D,E), no significant changes were observed between Utr(1−261) and Utr(28−261). The blue curve in panel B is the instrument response function (IRF) of the time-resolved fluorescence instrument. The inset in panel D shows the amide I region.

Table 1. Actin Binding Affinity Parameters Obtained from the Global Analysis of Three Independent Sets of Co-Sedimentation Assays (Figure 3) and Thermodynamic Stability Parameters Obtained from the Global Analysis of Six Denaturant Melts (Figure 4)

	$\Delta G_{NI} = \Delta G_{CH1} + \Delta G_{CH1-CH2}$ (kcal/mol)	$m_{NI} = m_{CH1} + m_{CH1-CH2}$ [kcal mol^{-1} (M urea)$^{-1}$]	$\Delta G_{IU} = \Delta G_{CH2}$ (kcal/mol)	$m_{IU} = m_{CH2}$ [kcal mol^{-1} (M urea)$^{-1}$]	K_d (μM)	B_{max}
Utr(1−261)	7.94 ± 0.39	−1.77 ± 0.09	5.13 ± 0.24	−0.95 ± 0.04	1.53 ± 0.88	0.85 ± 0.03
Utr(28−261)	9.31 ± 0.56	−2.23 ± 0.14	5.13 ± 0.24	−0.95 ± 0.04	45.52 ± 7.63	1.00 ± 0.10

Utr(1−261) and Utr(28−261) showed identical Stern−Volmer quenching plots (Figure 6A), indicating no effect of the N-terminal flanking region on the tertiary structure of the protein. In addition, we examined the time-resolved fluorescence intensity decay of full-length and truncated constructs (Figure 6B). Fluorescence lifetimes are much more sensitive to changes in the tryptophan local environment rather than the steady-state fluorescence intensity.[31] Utr(1−261) and Utr(28−261) exhibited identical time-resolved fluorescence decays (Figure 6B), indicating no major changes in the global tertiary structure of the protein.

We further used IR and Raman spectroscopy as orthogonal methods to monitor changes in the secondary and tertiary structures upon truncation. IR spectra did not show a significant change in the amide I region around 1650 cm^{-1} (Figure 6C). Similarly, Raman spectra are very similar within the experimental noise (Figure 6D). Individual Raman bands are characteristic of secondary structural changes around the peptide backbone as well as tertiary structural changes around

some of the key residues such as tyrosines and tryptophans.[34] No change in IR or Raman spectra indicates that the presence of the N-terminal flanking region did not significantly perturb the structure of the utrophin tandem CH domain.

Mechanism by Which the N-Terminal Flanking Region Modulates The Actin Binding Affinity of the Tandem CH Domain. The mechanism by which the N-terminal flanking region modules actin binding affinity might be purely modulation of the thermodynamic stability of the tandem CH domain, in particular, the CH1 domain. Results previously published by our group for utrophin and dystrophin tandem CH domains have shown that the CH1 domain primarily determines the actin binding function compared to the CH2 domain.[16,17] In addition, a surprising inverse relationship has been observed between the thermodynamic stability and actin binding function of tandem CH domains of utrophin,[19,35] dystrophin,[19] α-actinin,[36] filamin,[37] and spectrin.[38] Many mutations that destabilize the tandem CH domains have increased actin binding affinity compared to those of their

corresponding wild-type proteins. In addition, the tandem CH domains that exist in open conformations with minimal inter-CH-domain interactions bind to actin with affinities higher than those of closed conformations with significant inter-CH-domain interactions.[19] A similar mechanism may be functional in the case of the effect of the N-terminal flanking region on actin binding. The presence of the N-terminal flanking region destabilizes the CH1 domain (Figure 4 and Table 1). Utr(1−261) is less stable than Utr(28−261). However, destabilized Utr(1−261) binds to actin with an affinity higher than that of Utr(28−261). The change in binding free energy {$\Delta\Delta G_{\mathrm{bind}} = -RT \ln[K_{\mathrm{d,Utr(1-261)}}/K_{\mathrm{d,Utr(28-261)}}] = 1.99 \pm 0.35$ kcal/mol} is on the same order of magnitude as the change in unfolding free energy [$\Delta\Delta G_{\mathrm{unf}} = \Delta G_{\mathrm{unf,Utr(1-261)}} - \Delta G_{\mathrm{unf,Utr(28-261)}} = 1.37 \pm 0.68$ kcal/mol] within the error limits (propagation of errors calculated using formulas described previously[39]).

◼ DISCUSSION

Despite tandem CH domains being the most prevalent actin-binding domains in proteins,[1,2] structural principles underlying their actin binding are not clearly understood. An in-depth understanding of such structure−function aspects will help in developing better mini-proteins for treating muscle diseases using gene therapy. Dystrophin and utrophin are central to finding a cure for Duchenne/Becker muscular dystrophy. Our earlier results for their actin-binding tandem CH domains showed that CH1 is sufficient to bind to actin.[16,17] However, despite being highly similar in sequence and structure, the utrophin tandem CH domain binds to actin 30 times stronger than that of dystrophin. Here, we examined whether this difference in actin binding can be explained in terms of the differences in their N-terminal flanking regions that occur before the CH1 domains. We examined the effect of the N-terminal flanking region on the actin binding affinity of the utrophin tandem CH domain. We chose the utrophin tandem CH domain for two reasons: (i) it has one of the longest flanking region (27 residues) compared to others, and (ii) it exists in an open conformation with minimal inter-CH-domain interactions, so that we can probe the effect of the flanking region on CH1 that mainly controls the actin binding function. Deletion of the flanking region decreased the actin binding affinity of the utrophin tandem CH domain 30-fold, and the decreased binding affinity is very similar to that of the dystrophin tandem CH domain with a shorter linker. The mechanism by which the N-terminal flanking region enhances actin binding is not likely through its direct interaction with ABSs, but by decreasing the thermodynamic stability of the CH1 domain. This modulation of thermodynamic stability can occur through very weak structural interactions that may not be detectable by the spectroscopic techniques we employed here. In addition, it has been shown that attaching a completely unfolded random coil polypeptide chain to a well-folded globular domain can also affect the stability of the globular domain even when there is no other interaction between the two.[40]

Our results presented here, consistent with earlier results,[45] imply that the tandem CH domains with longer N-terminal flanking regions bind to actin more strongly than those with shorter flanking regions when their CH1 domains are identical. Further support for this hypothesis comes from published studies on the tandem CH domain of α-actinin.[15] In all tandem CH domains examined thus far, the sequence of the tandem CH domain of α-actinin is more similar to that of utrophin after

dystrophin.[22] It also has a longer N-terminal flanking region before the tandem CH domain. Similar to utrophin, the α-actinin tandem CH domain also binds to actin with an affinity ($K_{\mathrm{d}} = 4.3$ μM)[15] higher than that of dystrophin with a shorter N-terminal flanking region ($K_{\mathrm{d}} = 47.05 \pm 13.92$ μM).[16,19] Actin binding affinities of other tandem CH domains are difficult to attribute to their differences in their N-terminal flanking region, because their CH1 domains also differ significantly.

This study of the role of the N-terminal flanking regions along with our earlier studies of the contribution of individual CH domains[16,17,26] and inter-CH-domain linker[19] to the structure and function of tandem CH domains of dystrophin and utrophin may help in engineering better mini-dystrophins and mini-utrophins. Adeno virus-associated (AAV) gene therapies using shortened constructs of dystrophin and utrophin have been shown to compensate for the loss of functional dystrophin in human disease animal models;[5,6,41−43] however, these mini-proteins have not yet undergone the transition to therapies for the treatment of human patients. The major problems were decreased stability, decreased in vivo lifetime, and decreased function.[7−9,18] To design better gene constructs, we need to first understand what structural units are required for the stability and function of dystrophin and utrophin. Very little of this kind of information is available. So far, structure−function information is available for only one-fifth of the protein sequence. In this work and in our previous work,[16−20,26,30,44] we attempted to dissect the structural principles of actin binding function of dystrophin and utrophin tandem CH domains. The actin binding function is determined by the CH1 domains,[16,17] whereas the structural stability is determined by the CH2 domains.[16,26] The interdomain linker primarily determines the structural stability of tandem CH domains by modulating the inter-CH-domain interactions in terms of closed versus open conformations.[18,19] Closed conformations with significant inter-CH-domain interactions bind more weakly to actin than do open conformations with weakened inter-CH-domain interactions,[19,20] most probably because of the need to open the interface between the two CH domains for CH1 to bind to actin. The N-terminal flanking region affects actin binding by modulating the thermodynamic stability of the CH1 domain (this work). Combining these different structural elements from dystrophin and utrophin might lead to better chimeric constructs with improved function and stability.

◼ ASSOCIATED CONTENT

ⓢ Supporting Information

The Supporting Information is available free of charge on the ACS Publications website at DOI: 10.1021/acs.biochem.6b01117.

> Thermodynamic stability parameters obtained from the global analysis of denaturant melts (Figure 4) without the assumption that CH2 stability remains the same in Utr(1−261) and Utr(28−261) (Table S1) (PDF)

◼ AUTHOR INFORMATION

Corresponding Author

*Address: 12850 E. Montview Blvd., MS C238, Skaggs School of Pharmacy and Pharmaceutical Sciences, University of Colorado Anschutz Medical Campus, Aurora, CO 80045. E-mail: krishna.mallela@ucdenver.edu. Phone: 1-303-724-3576. Fax: 1-303-724-7266.

ORCID ⬤

Krishna M. G. Mallela: 0000-0001-8308-5318

■ ABBREVIATIONS

AUC, analytical ultracentrifugation; CD, circular dichroism; CH, calponin-homology; CH1, N-terminal CH; CH2, C-terminal CH; ΔG_{unf}, Gibbs free energy of unfolding; DLS, dynamic light scattering; IRF, instrument response function; K_d, dissociation constant; m-value, linear slope of ΔG_{unf} variation with denaturant concentration; TCSPC, time-correlated single-photon counting; Utr, utrophin; Utr(1−261), full-length utrophin tandem CH domain consisting of residues 1−261; Utr(28−261), utrophin tandem CH domain with the 27-residue N-terminal flanking region deleted; Utr(1−27), peptide corresponding to the N-terminal flanking region of the utrophin tandem CH domain.

■ REFERENCES

(1) Gimona, M., and Winder, S. J. (2008) The calponin homology (CH) domain. In *Protein Science Encyclopedia* (Fersht, A., Ed.) pp 1−16, Wiley-VCH Verlag GmbH & Co. KGaA, Weinheim, Germany.

(2) Sjöblom, B., Ylänne, J., and Djinović-Carugo, K. (2008) Novel structural insights into F-actin-binding and novel functions of calponin homology domains. *Curr. Opin. Struct. Biol. 18*, 702−708.

(3) Aartsma-Rus, A., van Deutekom, J. C. T., Fokkema, I. F., van Ommen, G.-J. B., and Den Dunnen, J. T. (2006) Entries in the Leiden Duchenne muscular dystrophy mutation database: An overview of mutation types and paradoxical cases that confirm the reading-frame rule. *Muscle Nerve 34*, 135−144.

(4) Kaplan, J. M., Kim, S. H., North, K. N., Rennke, H., Correia, L. A., Tong, H.-Q., Mathis, B. J., Rodríguez-Pérez, J.-C., Allen, P. G., Beggs, A. H., and Pollak, M. R. (2000) Mutations in ACTN4, encoding -actinin-4, cause familial focal segmental glomerulosclerosis. *Nat. Genet. 24*, 251−256.

(5) Muir, L. A., and Chamberlain, J. S. (2009) Emerging strategies for cell and gene therapy of the muscular dystrophies. *Expert Rev. Mol. Med. 11*, e18.

(6) Fairclough, R. J., Wood, M. J., and Davies, K. E. (2013) Therapy for Duchenne muscular dystrophy: renewed optimizm from genetic approaches. *Nat. Rev. Genet. 14*, 373−378.

(7) Deol, J. R., Danialou, G., Larochelle, N., Bourget, M., Moon, J. S., Liu, A. B., Gilbert, R., Petrof, B. J., Nalbantoglu, J., and Karpati, G. (2007) Successful compensation for dystrophin deficiency by a helper-dependent adenovirus expressing full-length utrophin. *Mol. Ther. 15*, 1767−1774.

(8) Henderson, D. M., Belanto, J. J., Li, B., Heun-Johnson, H., and Ervasti, J. M. (2011) Internal deletion compromises the stability of dystrophin. *Hum. Mol. Genet. 20*, 2955−2963.

(9) Le Rumeur, E., Winder, S. J., and Hubert, J.-F. (2010) Dystrophin: More than just the sum of its parts. *Biochim. Biophys. Acta, Proteins Proteomics 1804*, 1713−1722.

(10) Levine, B. A., Moir, A. J., Patchell, V. B., and Perry, S. V. (1992) Binding sites involved in the interaction of actin with the N-terminal region of dystrophin. *FEBS Lett. 298*, 44−48.

(11) Levine, B. A., Moir, A. J., Patchell, V. B., and Perry, S. V. (1990) The interaction of actin with dystrophin. *FEBS Lett. 263*, 159−162.

(12) Winder, S. J., Knight, A. E., and Kendrick-Jones, J. (1997) Protein Structure. In *Dystrophin: Gene, protein and cell biology* (Brown, S. C., and Lucy, J. A., Eds.) pp 27−55, Cambridge University Press, Cambridge, U.K.

(13) Winder, S. J., Hemmings, L., Maciver, S. K., Bolton, S. J., Tinsley, J. M., Davies, K. E., Critchley, D. R., and Kendrick-Jones, J. (1995) Utrophin actin binding domain: analysis of actin binding and cellular targeting. *J. Cell Sci. 108* (Part 1), 63−71.

(14) Morris, G. E., Man, N. T., Huyen, N. t. N., Pereboev, A., Kendrick-Jones, J., and Winder, S. J. (1999) Disruption of the utrophin-actin interaction by monoclonal antibodies and prediction of an actin-binding surface of utrophin. *Biochem. J. 337* (1), 119−123.

(15) Way, M., Pope, B., and Weeds, A. G. (1992) Evidence for functional homology in the F-actin binding domains of gelsolin and α-actinin: Implications for the requirements of severing and capping. *J. Cell Biol. 119*, 835−842.

(16) Singh, S. M., Bandi, S., and Mallela, K. M. G. (2015) The N- and C-terminal domains differentially contribute to the structure and function of dystrophin and utrophin tandem calponin-homology domains. *Biochemistry 54*, 6942−6950.

(17) Singh, S. M., Bandi, S., Winder, S. J., and Mallela, K. M. G. (2014) The actin binding affinity of the utrophin tandem calponin-homology domain is primarily determined by its N-terminal domain. *Biochemistry 53*, 1801−1809.

(18) Singh, S. M., Molas, J. F., Kongari, N., Bandi, S., Armstrong, G. S., Winder, S. J., and Mallela, K. M. G. (2012) Thermodynamic stability, unfolding kinetics, and aggregation of the N-terminal actin-binding domains of utrophin and dystrophin. *Proteins: Struct., Funct., Genet. 80*, 1377−1392.

(19) Bandi, S., Singh, S. M., and Mallela, K. M. G. (2015) Interdomain linker determines primarily the structural stability of dystrophin and utrophin tandem calponin-homology domains rather than their actin-binding affinity. *Biochemistry 54*, 5480−5488.

(20) Singh, S. M., and Mallela, K. M. G. (2012) The N-terminal actin-binding tandem calponin-homology (CH) domain of dystrophin is in a closed conformation in solution and when bound to F-actin. *Biophys. J. 103*, 1970−1978.

(21) Lin, A. Y., Prochniewicz, E., James, Z. M., Svensson, B., and Thomas, D. D. (2011) Large-scale opening of utrophin's tandem calponin homology (CH) domains upon actin binding by an induced-fit mechanism. *Proc. Natl. Acad. Sci. U. S. A. 108*, 12729−12733.

(22) Norwood, F. L. M., Sutherland-Smith, A. J., Keep, N. H., and Kendrick-Jones, J. (2000) The structure of the N-terminal actin-binding domain of human dystrophin and how mutations in this domain may cause Duchenne or Becker muscular dystrophy. *Structure 8*, 481−491.

(23) Mossessova, E., and Lima, C. D. (2000) Ulp1-SUMO crystal structure and genetic analysis reveal conserved interactions and a regulatory element essential for cell growth in yeast. *Mol. Cell 5*, 865−876.

(24) Greenfield, N. J. (2007) Using circular dichroism spectra to estimate protein secondary structure. *Nat. Protoc. 1*, 2876−2890.

(25) Bilsel, O., Zitzewitz, J. A., Bowers, K. E., and Matthews, C. R. (1999) Folding mechanism of the α-subunit of tryptophan synthase, an α/β barrel protein: global analysis highlights the interconversion of multiple native, intermediate, and unfolded forms through parallel channels. *Biochemistry 38*, 1018−1029.

(26) Bandi, S., Singh, S. M., and Mallela, K. M. G. (2014) The C-terminal domain of the utrophin tandem calponin-homology domain appears to be thermodynamically and kinetically more stable than the full-length protein. *Biochemistry 53*, 2209–2211.

(27) Chen, Y., and Barkley, M. D. (1998) Toward understanding tryptophan fluorescence in proteins. *Biochemistry 37*, 9976–9982.

(28) Royer, C. A. (2006) Probing protein folding and conformational transitions with fluorescence. *Chem. Rev. 106*, 1769–1784.

(29) Tal, M., Silberstein, A., and Nusser, E. (1985) Why does Coomassie Brilliant Blue R interact differently with different proteins? A partial answer. *J. Biol. Chem. 260*, 9976–9980.

(30) Singh, S. M., Bandi, S., Shah, D. D., Armstrong, G., and Mallela, K. M. G. (2014) Missense mutation Lys18Asn in dystrophin that triggers X-linked dilated cardiomyopathy decreases protein stability, increases protein unfolding, and perturbs protein structure, but does not affect protein function. *PLoS One 9*, e110439.

(31) Lakowicz, J. R. (2006) *Principles of Fluorescence Spectroscopy*, 3rd ed., Springer Science, New York.

(32) Santoro, M. M., and Bolen, D. W. (1992) A test of the linear extrapolation of unfolding free energy changes over an extended denaturant concentration range. *Biochemistry 31*, 4901–4907.

(33) Santoro, M. M., and Bolen, D. W. (1988) Unfolding free energy changes determined by the linear extrapolation method. 1. Unfolding of phenylmethanesulfonyl alpha-chymotrypsin using different denaturants. *Biochemistry 27*, 8063–8068.

(34) Wen, Z. Q. (2007) Raman spectroscopy of protein pharmaceuticals. *J. Pharm. Sci. 96*, 2861–2878.

(35) Broderick, M. J., Bobkov, A., and Winder, S. J. (2012) Utrophin ABD binds to F-actin in an open conformation. *FEBS Open Bio 2*, 6–11.

(36) Weins, A., Schlondorff, J. S., Nakamura, F., Denker, B. M., Hartwig, J. H., Stossel, T. P., and Pollak, M. R. (2007) Disease-associated mutant alpha-actinin-4 reveals a mechanism for regulating its F-actin-binding affinity. *Proc. Natl. Acad. Sci. U. S. A. 104*, 16080–16085.

(37) Sawyer, G. M., Clark, A. R., Robertson, S. P., and Sutherland-Smith, A. J. (2009) Disease-associated substitutions in the filamin B actin binding domain confer enhanced actin binding affinity in the absence of major structural disturbance: Insights from the crystal structures of filamin B actin binding domains. *J. Mol. Biol. 390*, 1030–1047.

(38) Avery, A. W., Crain, J., Thomas, D. D., and Hays, T. S. (2016) A human beta-III-spectrin spinocerebellar ataxia type 5 mutation causes high-affinity F-actin binding. *Sci. Rep. 6*, 21375.

(39) Bevington, P. R., and Robinson, D. K. (2003) *Data Reduction and Error Analysis for the Physical Sciences*, 3rd ed., McGraw-Hill, New York.

(40) Arviv, O., and Levy, Y. (2012) Folding of multidomain proteins: Biophysical consequences of tethering even in apparently independent folding. *Proteins: Struct., Funct., Genet. 80*, 2780–2798.

(41) Wang, B., Li, J., and Xiao, X. (2000) Adeno-associated virus vector carrying human minidystrophin genes effectively ameliorates muscular dystrophy in *mdx* mouse model. *Proc. Natl. Acad. Sci. U. S. A. 97*, 13714–13719.

(42) Gregorevic, P., Allen, J. M., Minami, E., Blankinship, M. J., Haraguchi, M., Meuse, L., Finn, E., Adams, M. E., Froehner, S. C., Murry, C. E., and Chamberlain, J. S. (2006) rAAV6-microdystrophin preserves muscle function and extends lifespan in severely dystrophic mice. *Nat. Med. 12*, 787–789.

(43) Odom, G. L., Gregorevic, P., Allen, J. M., Finn, E., and Chamberlain, J. S. (2008) Microutrophin delivery through rAAV6 increases lifespan and improves muscle function in dystrophic dystrophin/utrophin-deficient mice. *Mol. Ther. 16*, 1539–1545.

(44) Singh, S. M., Kongari, N., Cabello-Villegas, J., and Mallela, K. M. G. (2010) Missense mutations in dystrophin that trigger muscular dystrophy decrease protein stability and lead to cross-β aggregates. *Proc. Natl. Acad. Sci. U. S. A. 107*, 15069–15074.

(45) Moores, C. A., and Kendrick-Jones, J. (2000) Biochemical characterization of the actin-binding properties of utrophin. *Cell Motil. Cytoskeleton 46*, 116–128.